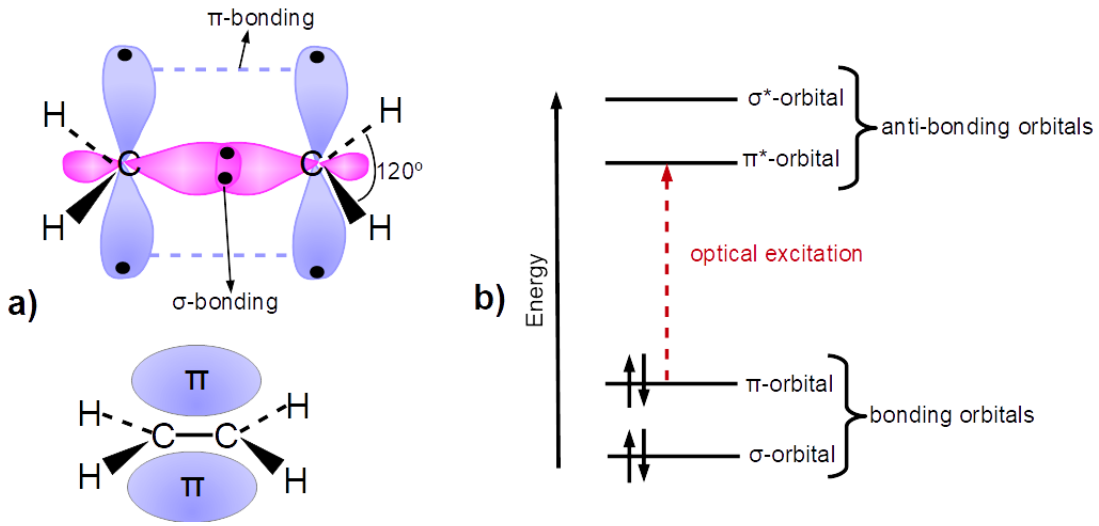

Figure 2.1: (a) σ- and π- bonds in ethane, as an example of the simplest conjugated π-electron system, (b) Energy level of a π-conjugated molecule where the lowest electronic excitation is between the bonding π-orbital and the antibonding π^*-orbital

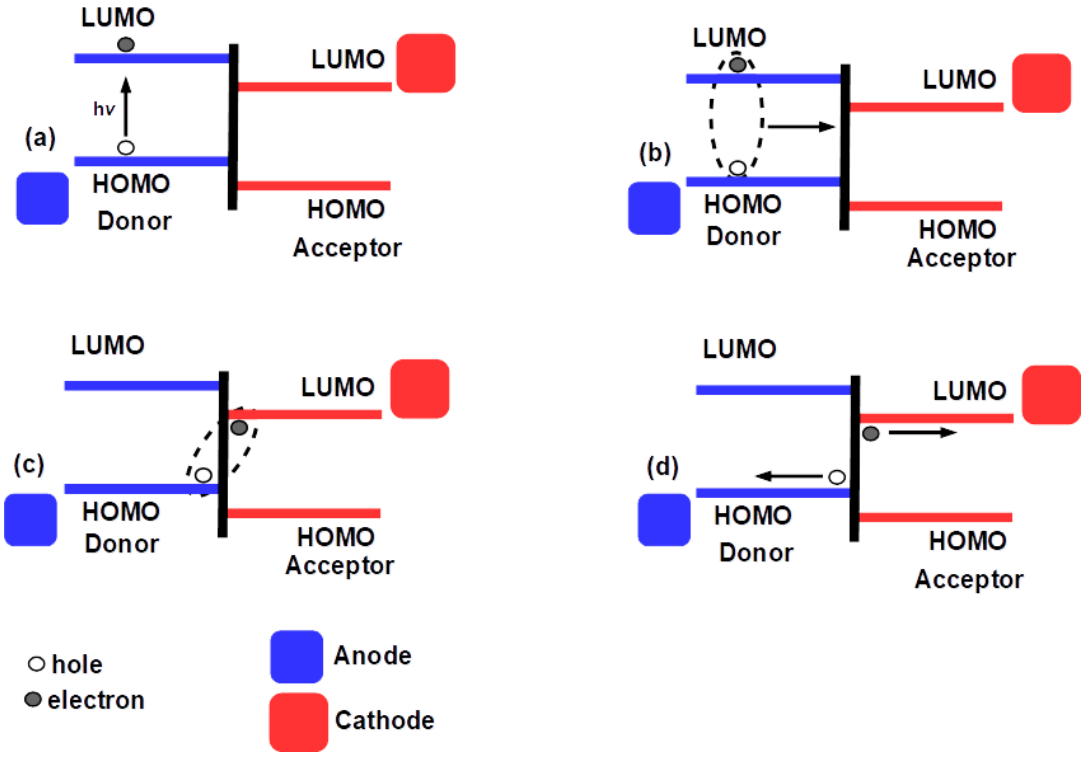

Figure 2.2: Schematic diagram of the working principle of OSCs

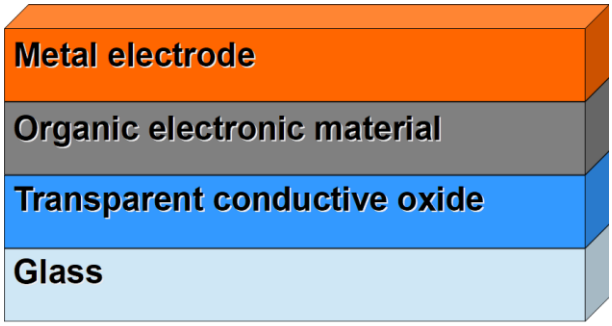

Figure *2.3:* Single layer

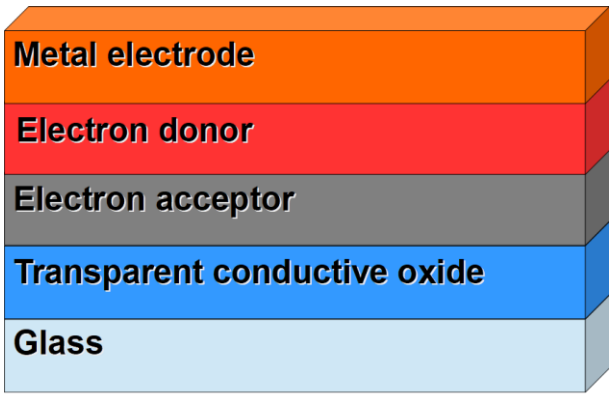

Figure *2.4:* Bilayer heterojunction

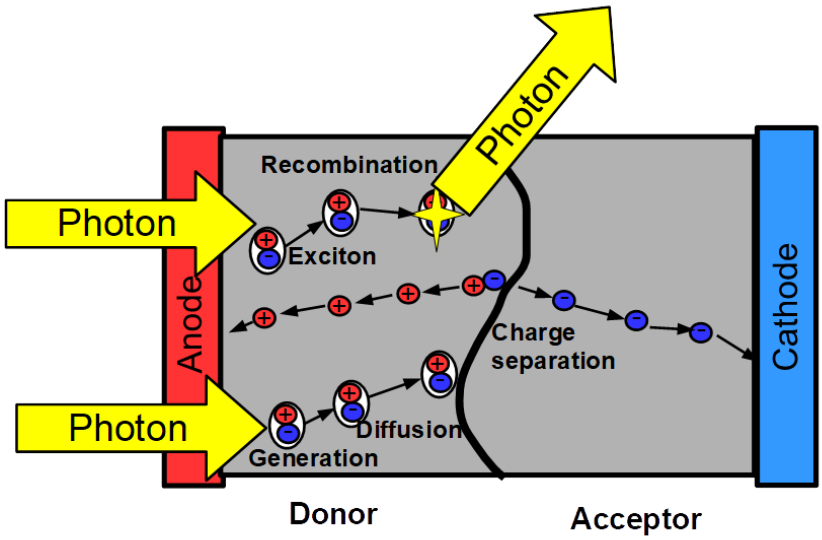

Figure *2.5:* Charge transfer in bilayer OSC

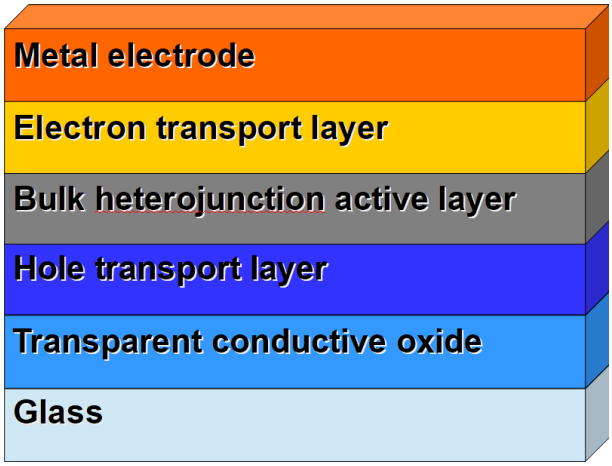

Figure *2.6:* Bulk heterojunction

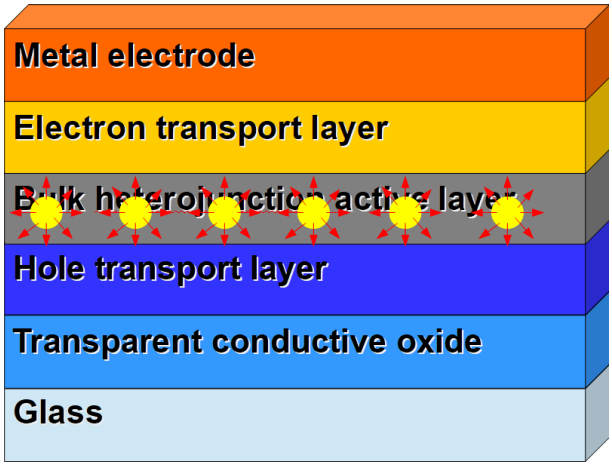

Figure *2.7:* Architecture of OSCs with NPs embedded inside the organic active layer

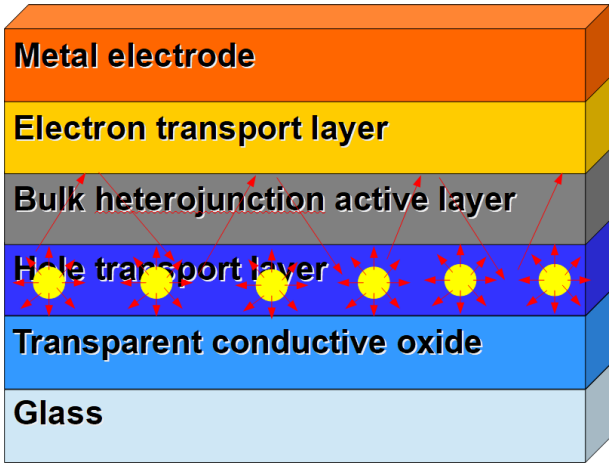

Figure *2.8:* Architecture of OSC with NPs embedded inside the CTL

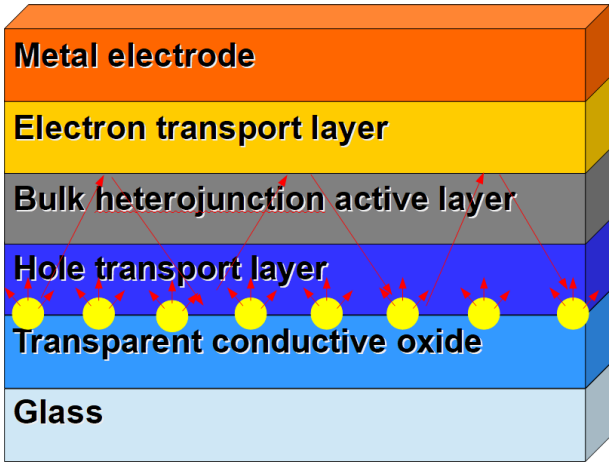

Figure *2.9:* Architecture of OSCs with NPs embedded at the TCO/CTL interface

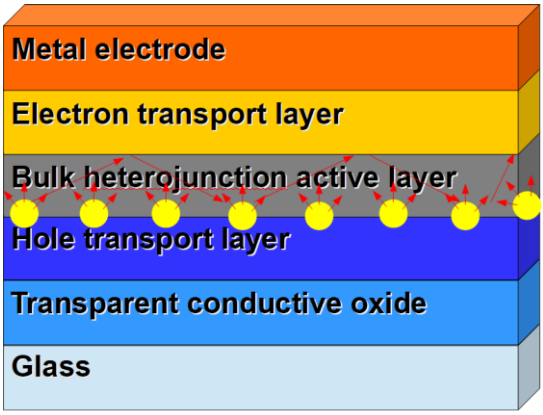

Figure *2.10:* Architecture of OSCs with NPs embedded at the CTL/active layer interface

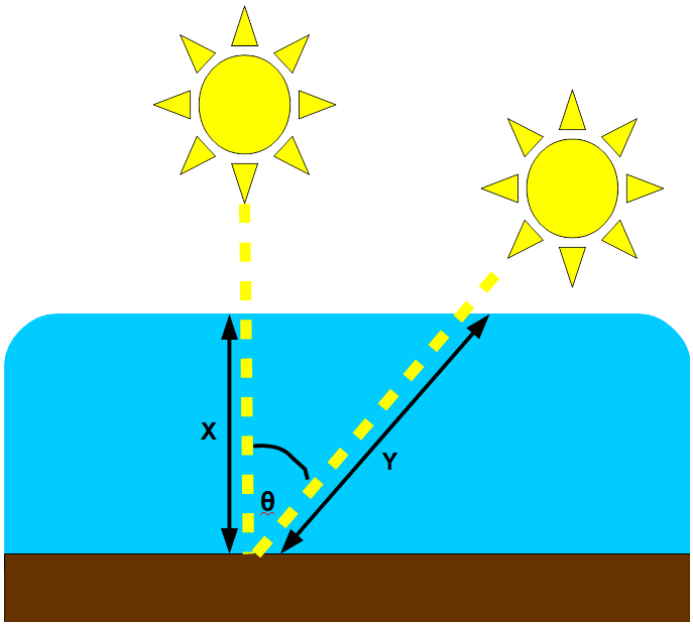

Figure *2.11:* Schematic diagram showing the proportion of atmosphere that the light must pass through before striking the Earth

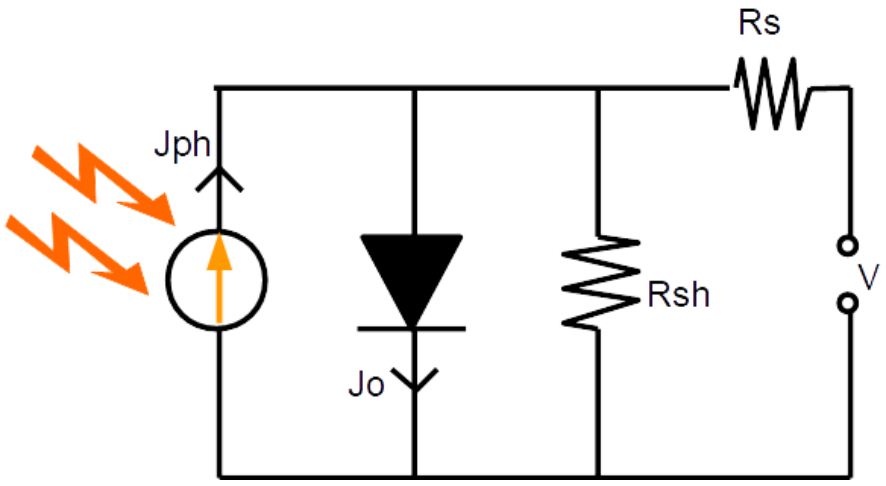

Figure *2.12:* Equivalent circuit of a solar cell

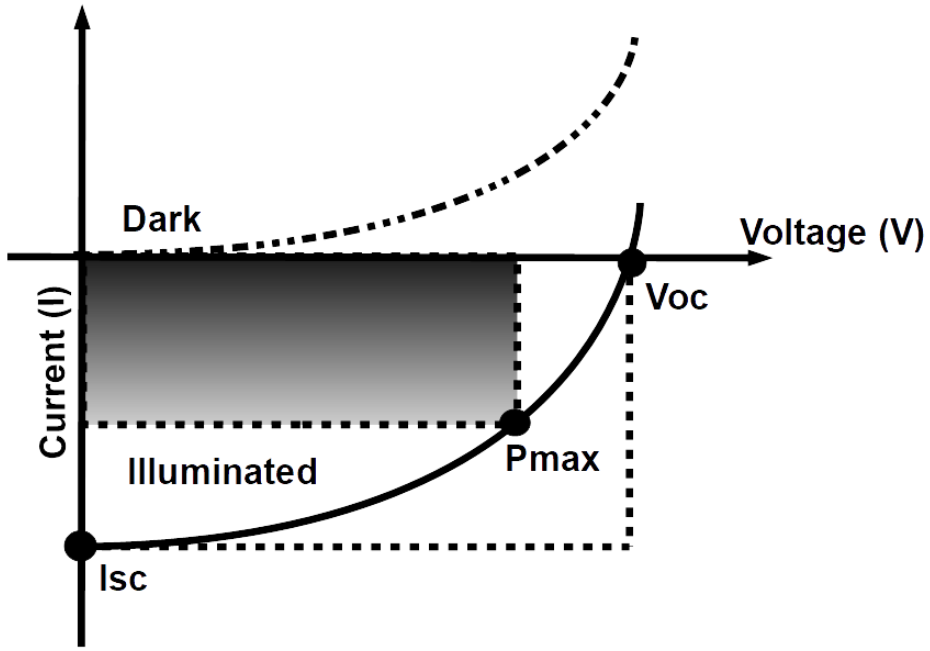

Figure *2.13:* Typical current-voltage response of a solar cell

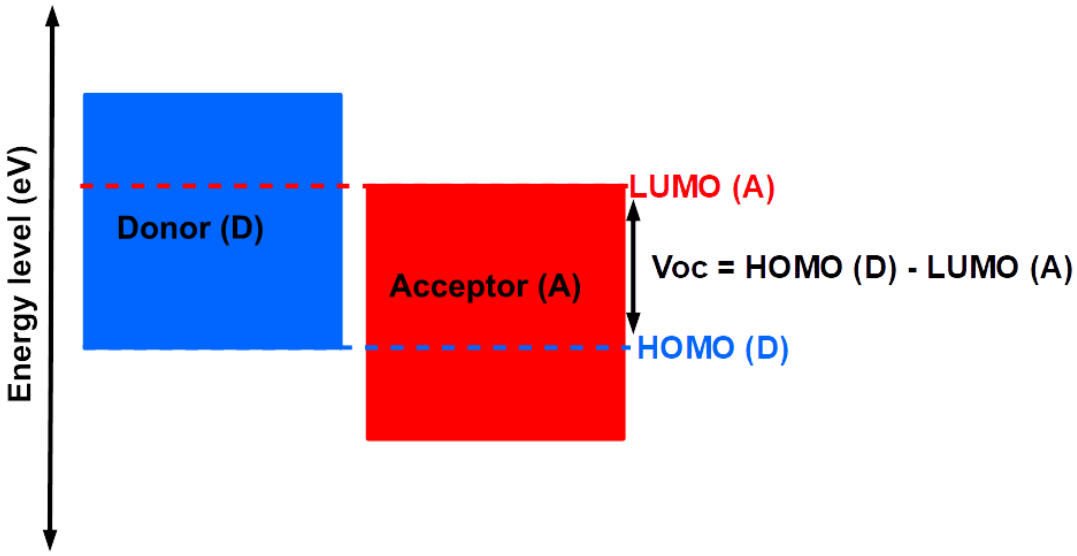

Figure 2.14: Schematic diagram showing the theoretical value $V_{OC,}$ which is determined by the energy difference between acceptor LUMO

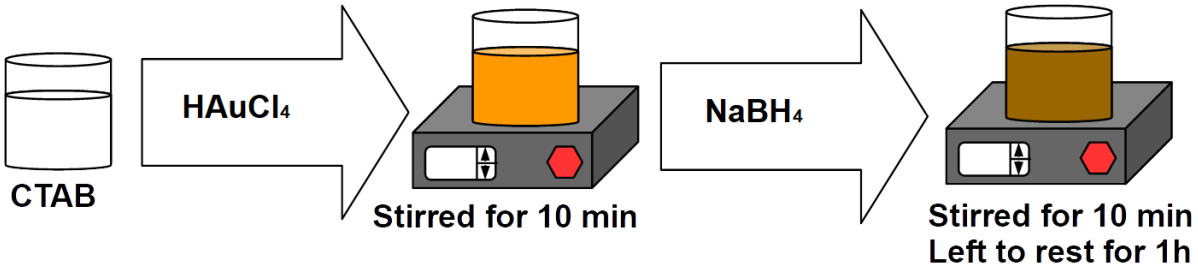

Figure 3.15: Schematic diagram illustrating the synthesis of gold-seed solution

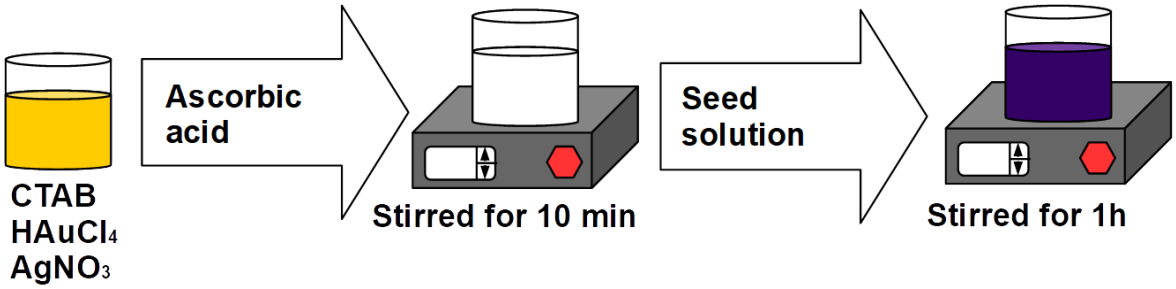

Figure 3.16: Schematic diagram showing the synthesis of gold nanorods

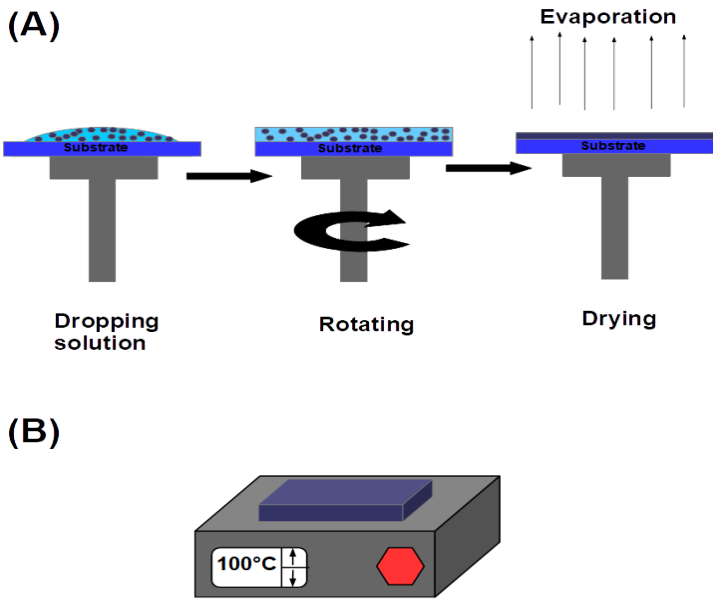

Figure 3.17: Schematic representation of (A) the spin-coating process and principle (B) drying of samples using a hot plate

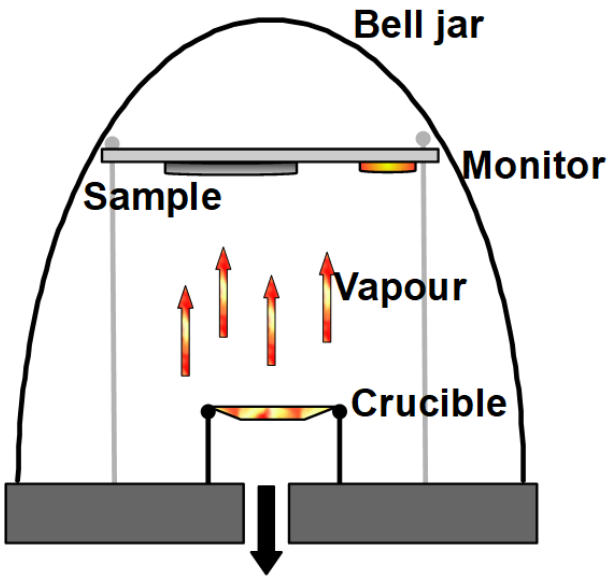

Figure 3.18: Schematic diagram of the thermal evaporation deposition system

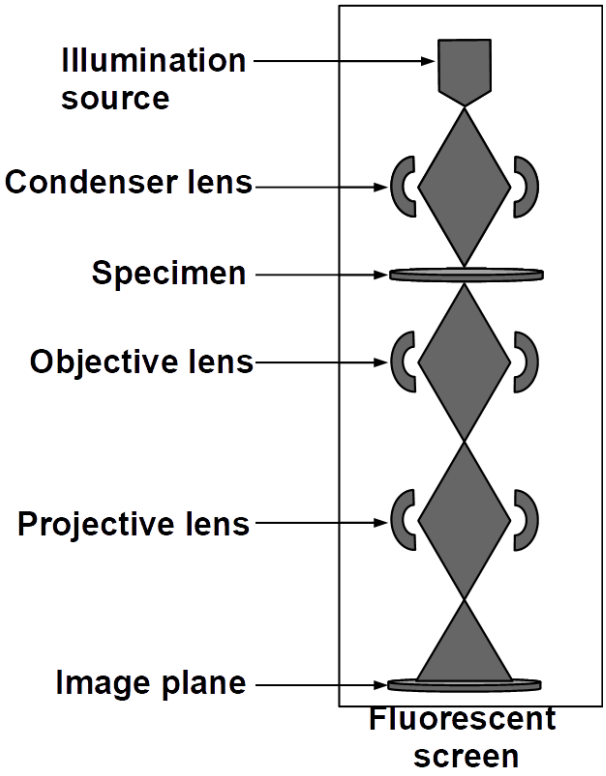

Figure 3.19: Schematic diagram of transmission electron microscopy

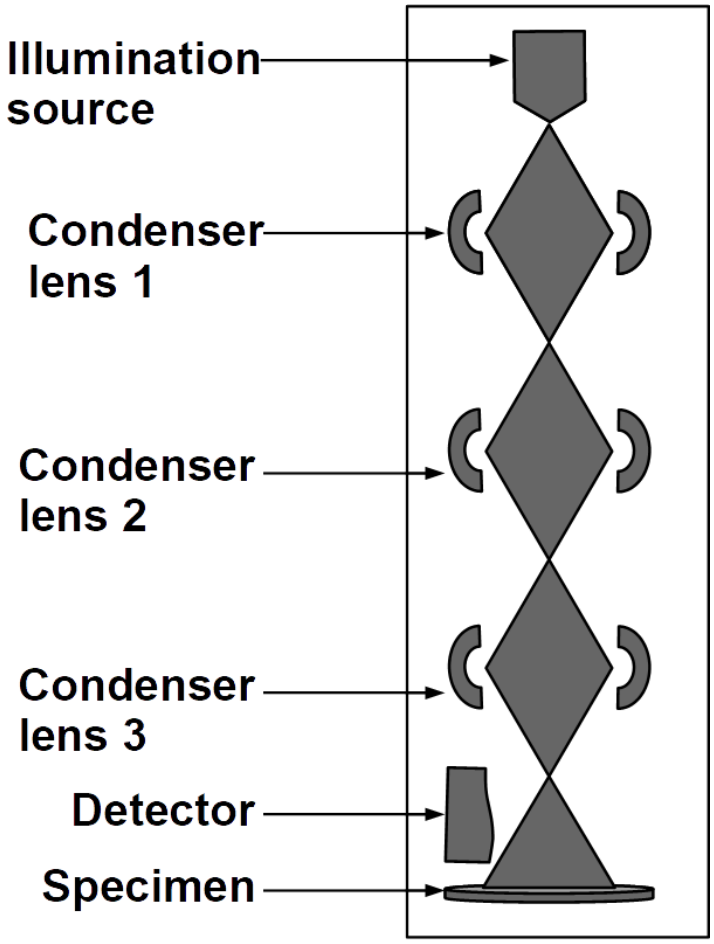

Figure 3.20: Schematic diagram of scanning electron microscopy

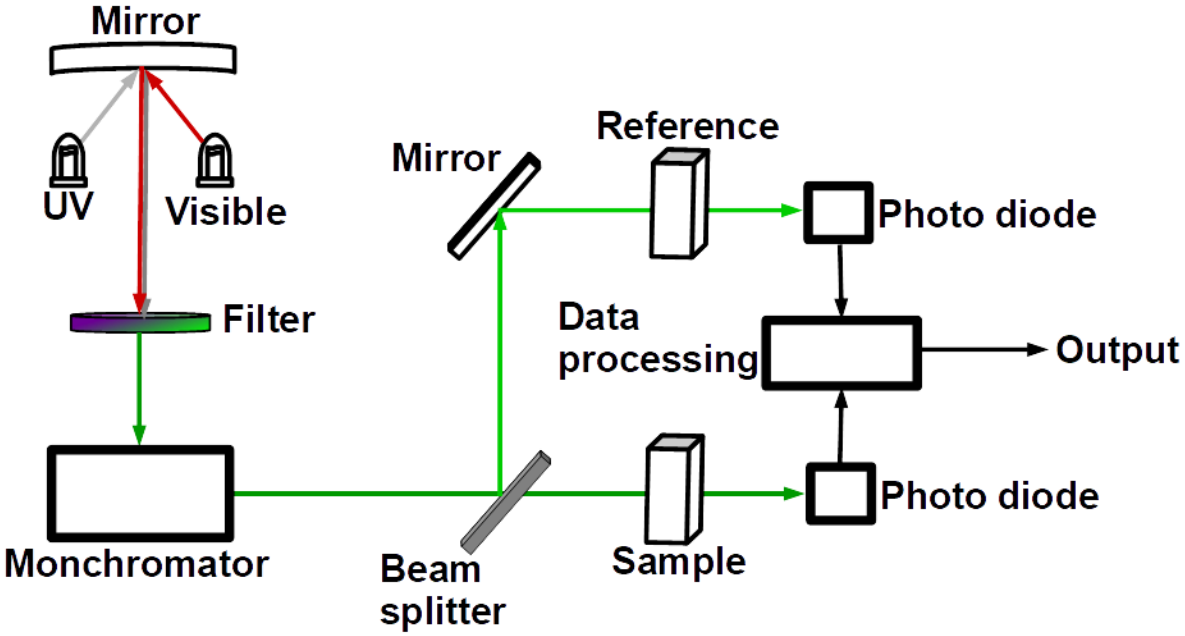

Figure 3.21: Schematic diagram of ultraviolet-visible spectroscopy

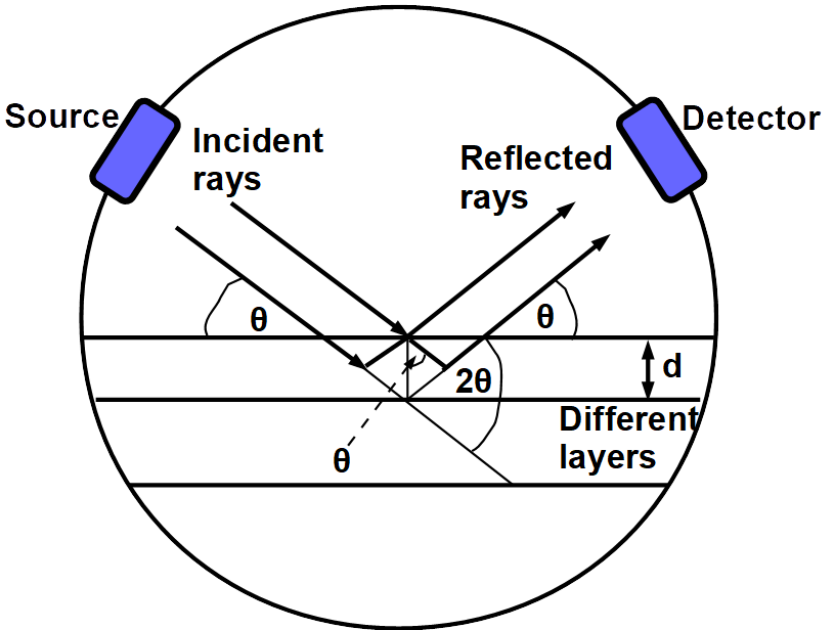

Figure 3.22: Schematic diagram of X-ray diffraction

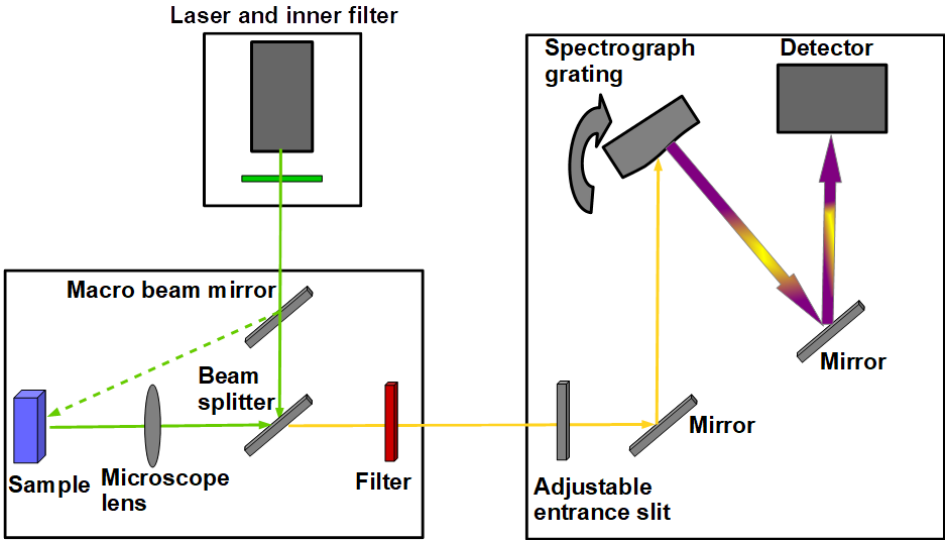

Figure 3.23: Schematic diagram showing the components of Raman spectroscopy

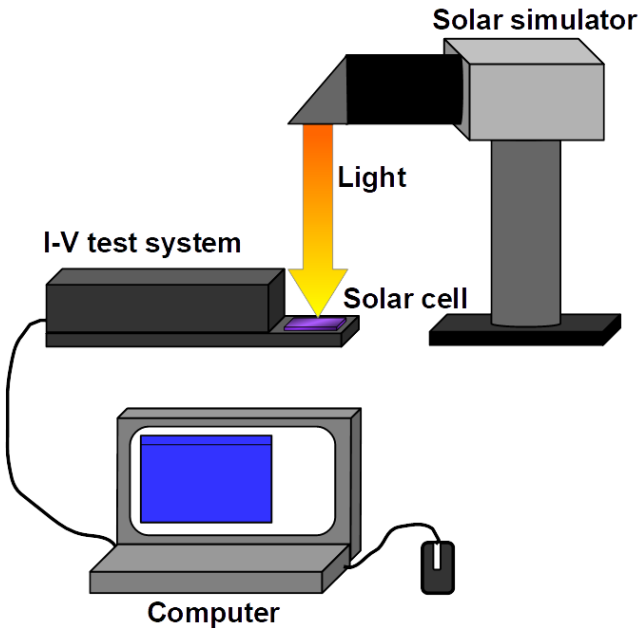

Figure 3.24: Schematic diagram of the solar simulator and Ossila I-V test system connected to a computer

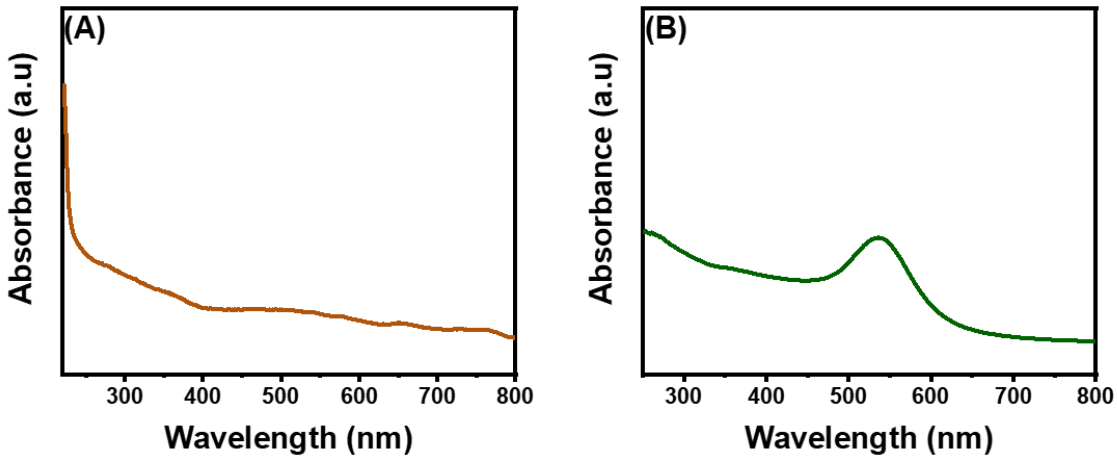

Figure 4.25: UV–Vis absorption spectrum of Au seeds (A) 12 h after synthesis and (B) after one week

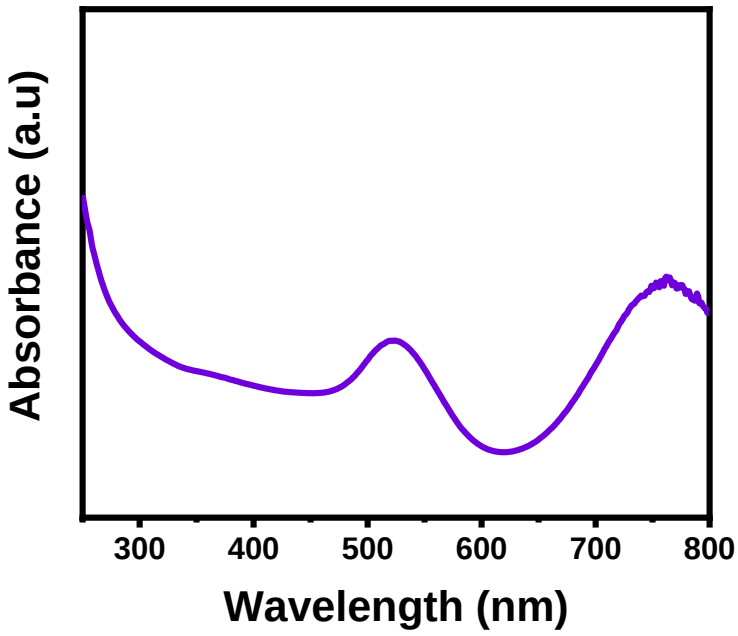

Figure 4.*26*: UV–Vis absorption spectrum of gold nanorods

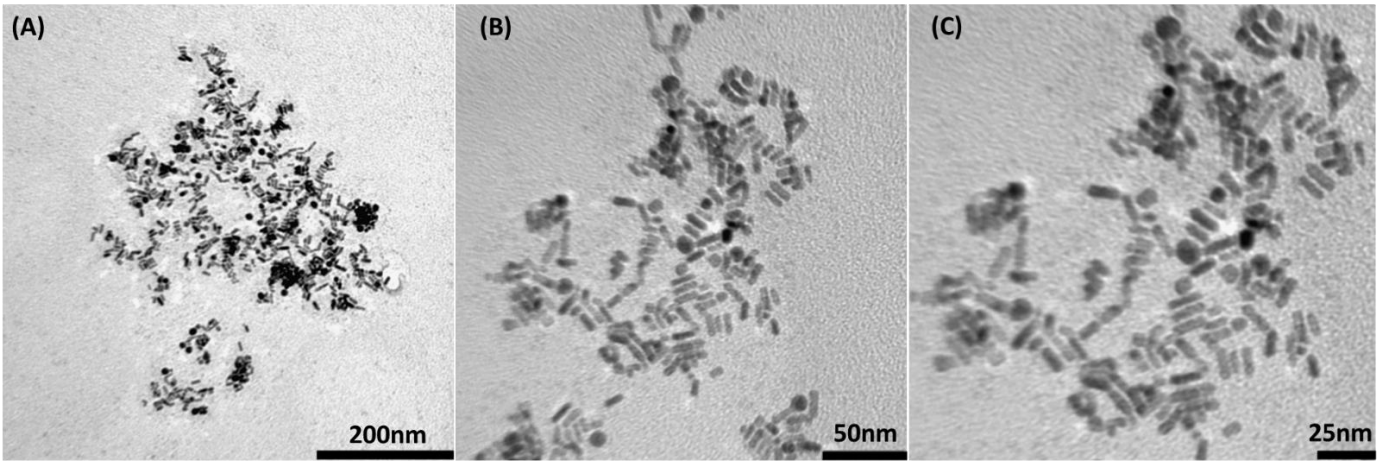

Figure 4.*27*:TEM images of gold nanorods

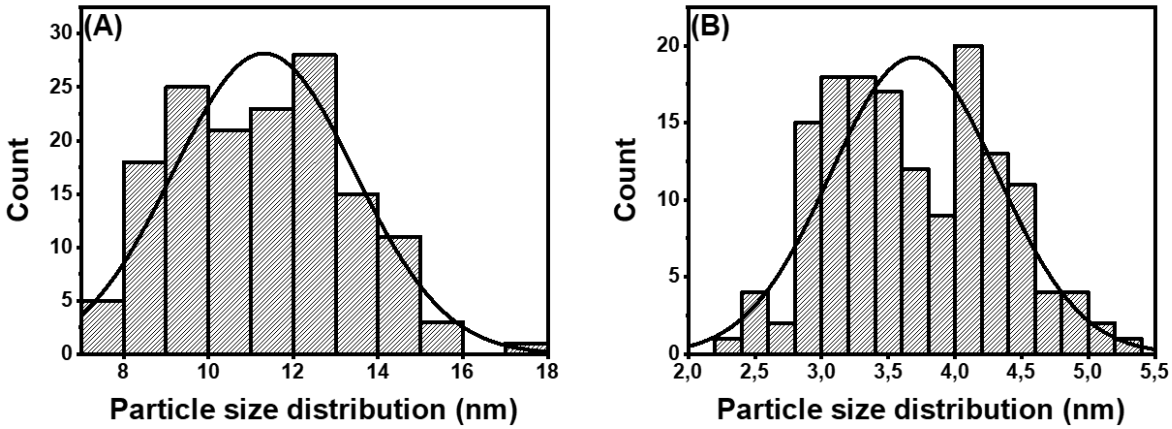

Figure 4.28: (A) Gold nanorod length distribution (B) Gold nanorod width distribution

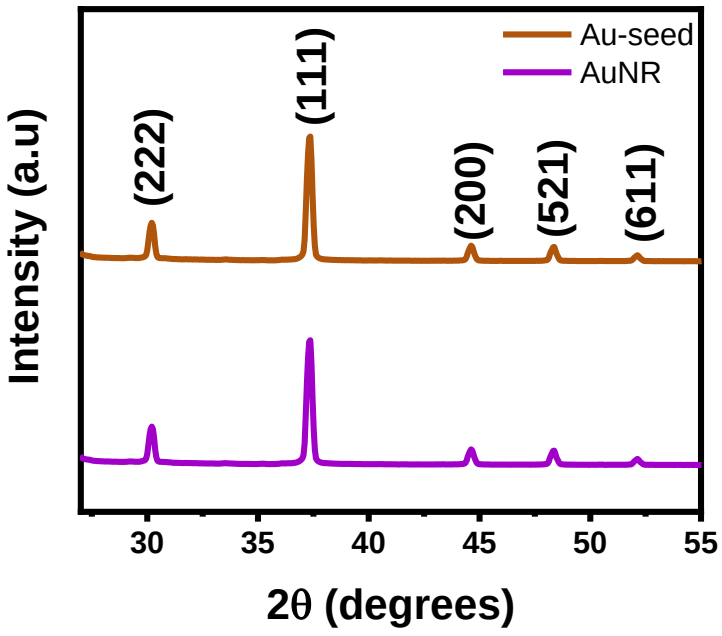

Figure 4.29: XRD pattern of gold nanorods and gold seed

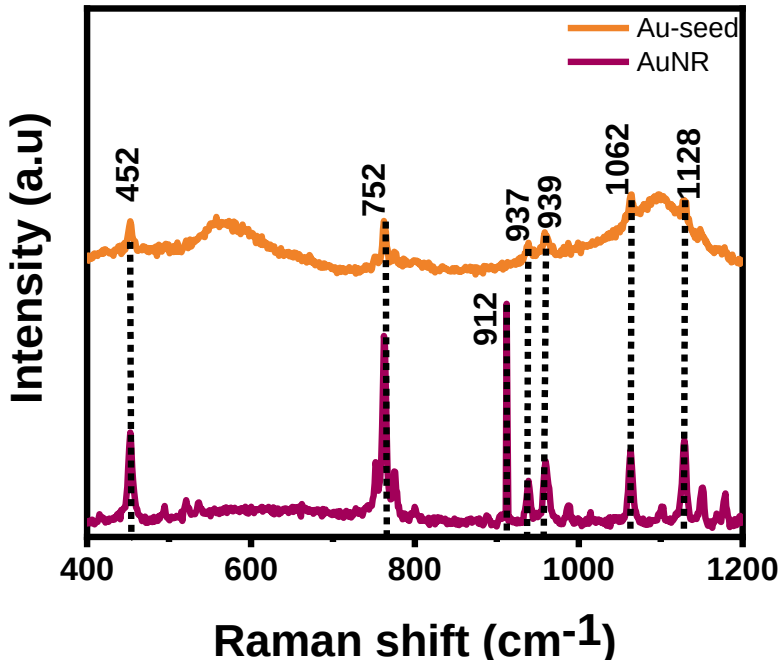

Figure 4.*30*: Raman spectra of gold nanorods and gold seeds

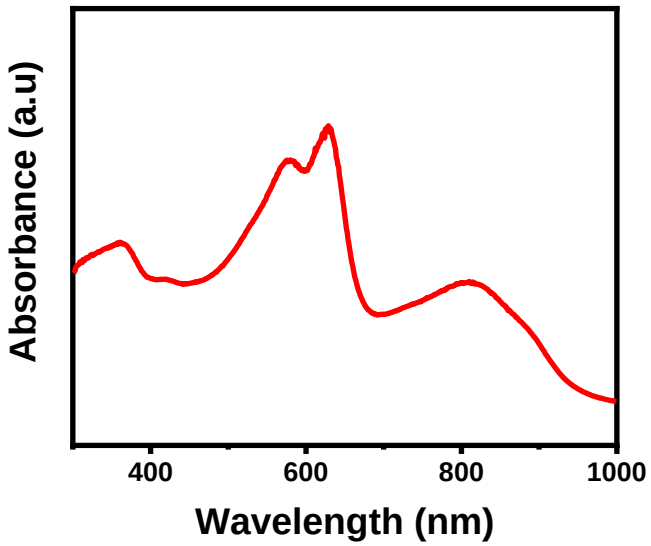

Figure 4.*31*: UV–Vis absorption spectrum of PM6:Y6

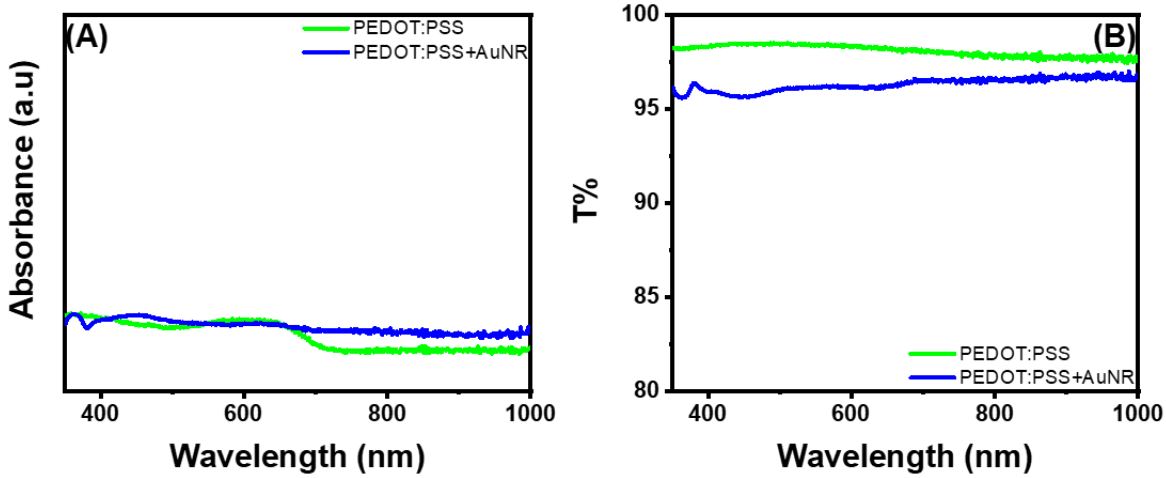

Figure 4.*32*: (A) UV–Vis absorption spectrum and (B) transmittance spectrum

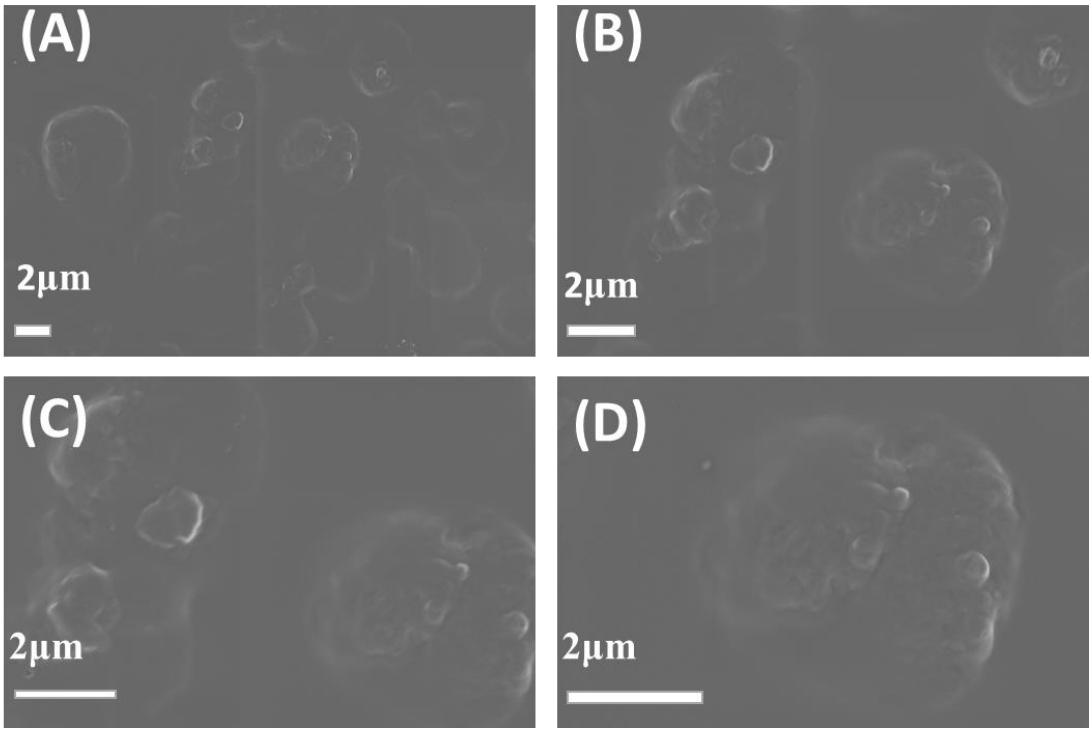

Figure 4.*33*: SEM images of PM6:Y6 with solvent additive

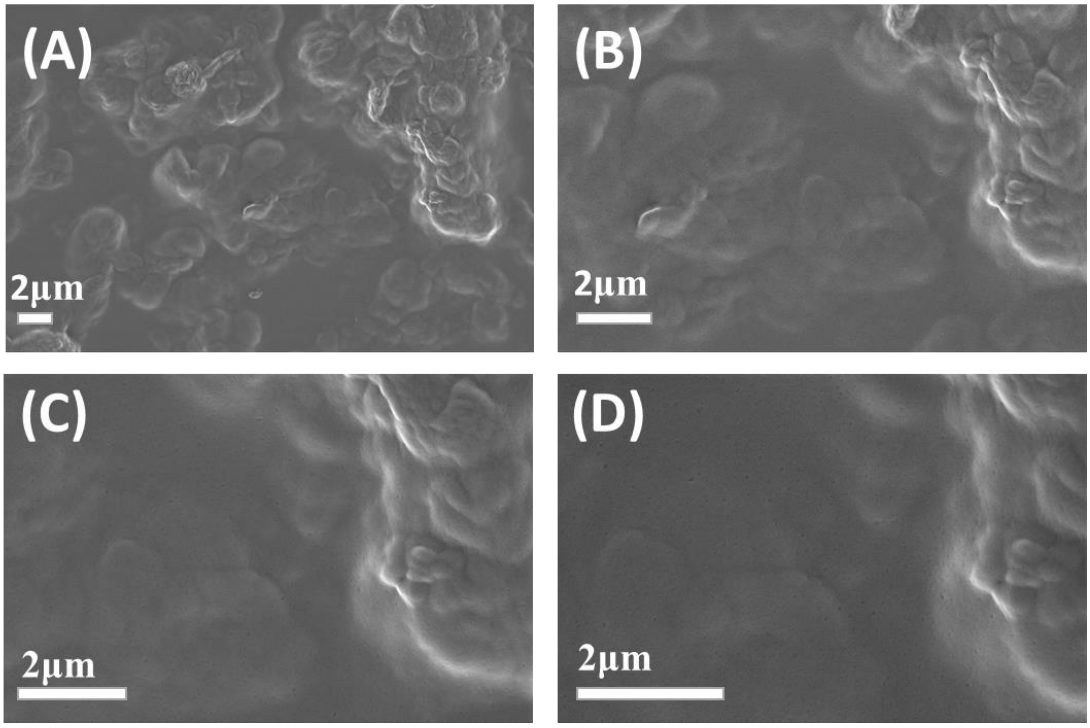

Figure 4.*34*: SEM images of PM6:Y6 without solvent additive

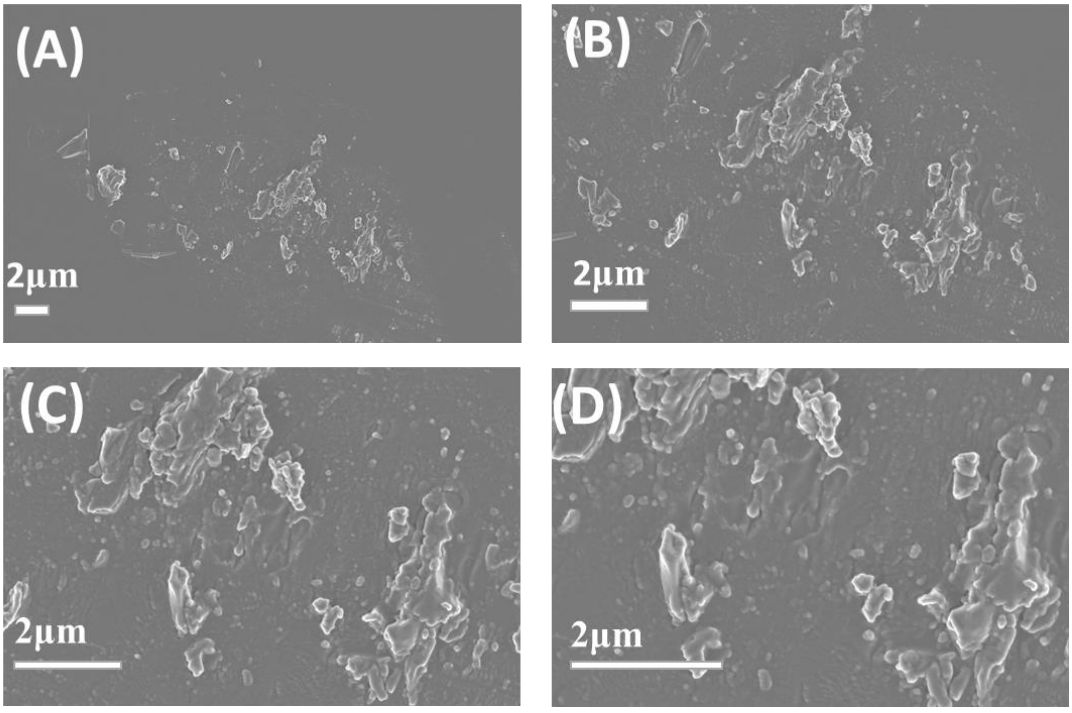

Figure 4.*35*: SEM images of PEDOT:PSS

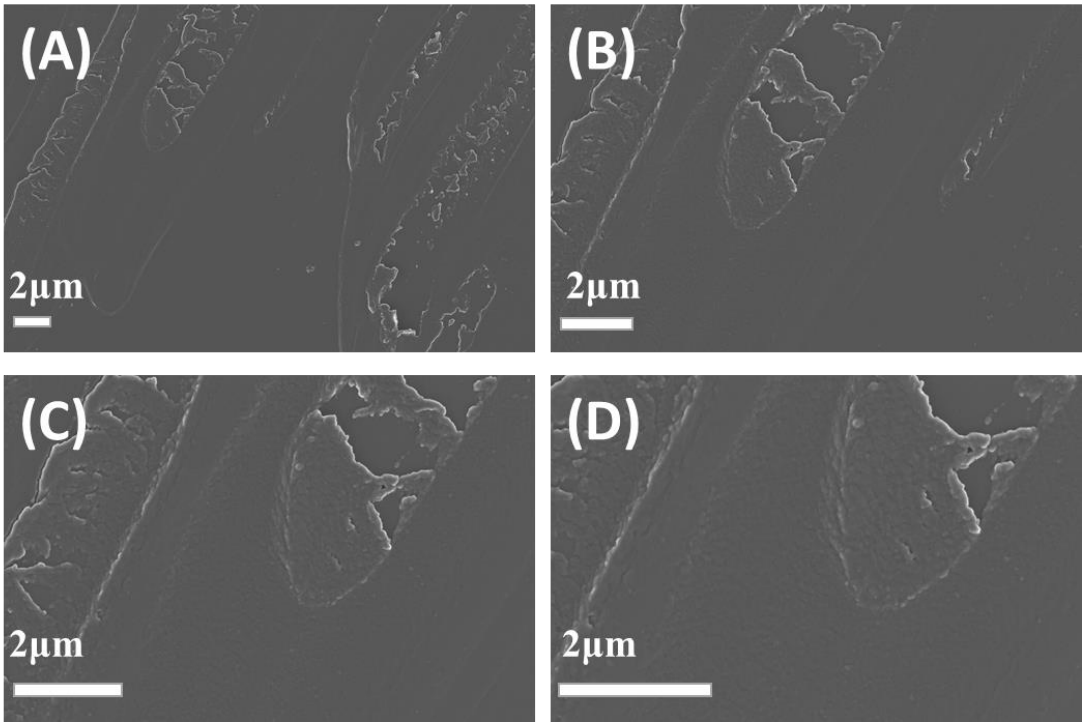

Figure 4.*36*: SEM images of PEDOT:PSS plus AuNR

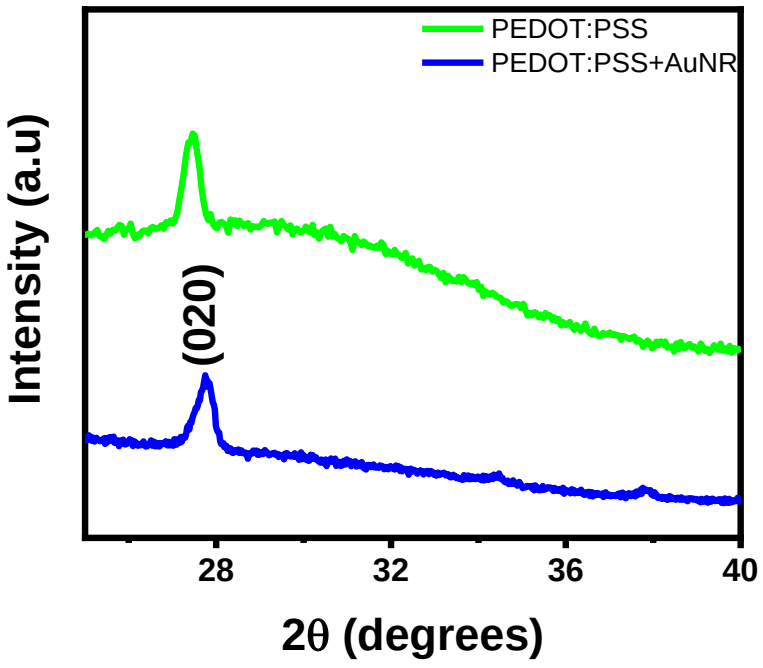

Figure 4.*37*: XRD patterns of PEDOT:PSS and PEDOT:PSS plus AuNRs

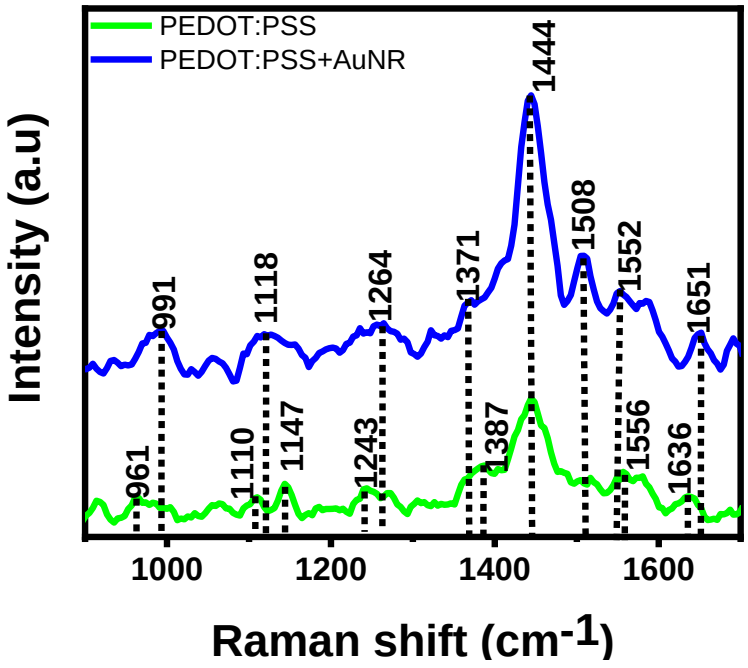

Figure 4.*38*: Raman spectra of PEDOT:PSS and PEDOT:PSS plus AuNRs

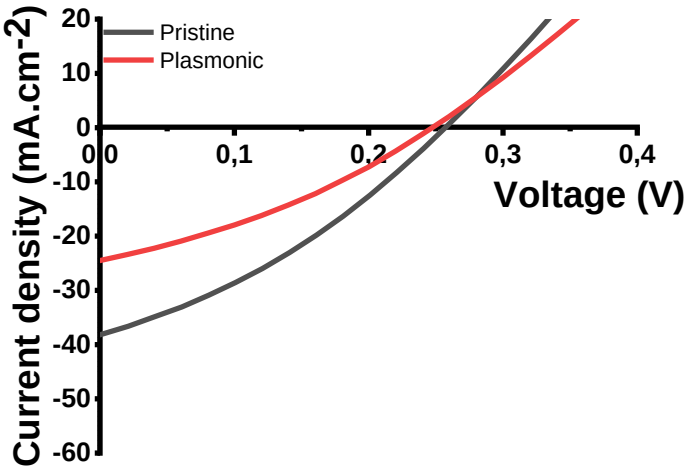

Figure 4.*39*: J-V of pristine and plasmonic device

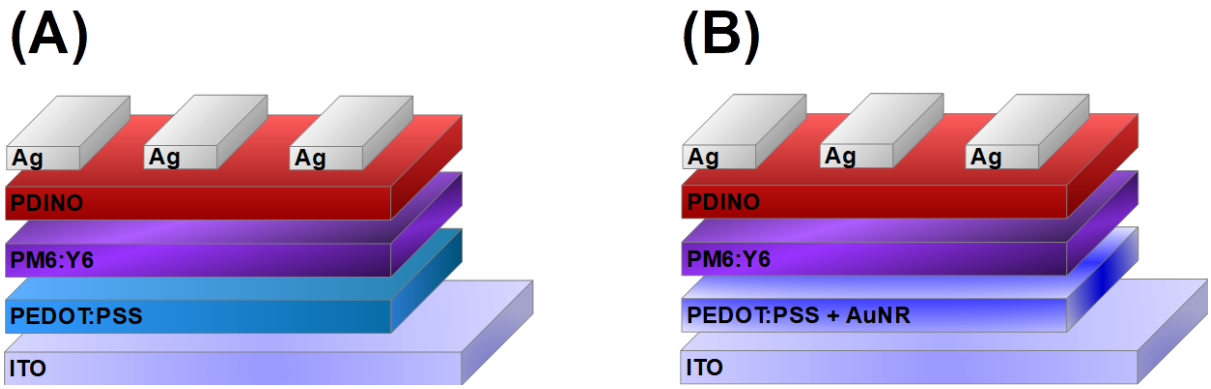

Figure 4.*40*: Schematic diagram of (A) pristine and (B) plasmonic devices

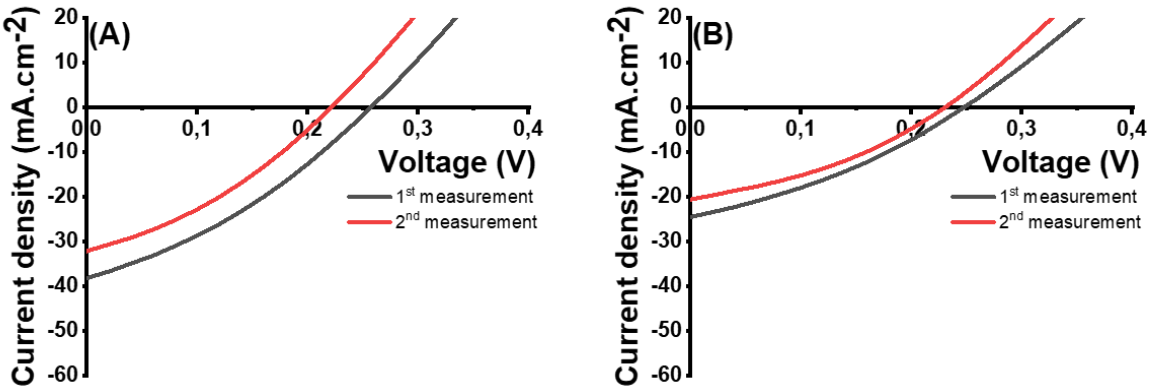

Figure 4.*41*: Degradation of (A) pristine and (B) plasmonic devices

Table 4.1: Photovoltaic parameters of pristine and plasmonic devices under illumination

Device	J_{sc} ($mAcm^{-2}$)	V_{oc} (V)	FF (%)	PCE (%)	R_s (Ωcm^2)
Pristine	36.68 ± 1.09	0.258 ± 0.01	33.1 ± 0.3	3.135 ± 0.113	4.475 ± 0.275
Plasmonic	24.315 ± 0.015	0.255 ± 0.05	33.35 ± 0.12	2.053 ± 0.052	6.215 ± 0.085

Table 4.2: Photovoltaic parameters of pristine and plasmonic devices under illumination for the 1st and 2nd measurements

Device	Measurement	J_{sc} ($mAcm^{-2}$)	V_{oc} (V)	FF (%)	PCE (%)	R_s (Ωcm^2)
Pristine	1st	36.68 ± 1.09	0.258 ± 0.01	33.1 ± 0.3	3.135 ± 0.113	4.475 ± 0.275
	2nd	30.935 ± 0.745	0.2255 ± 0.0035	34.15 ± 0.01	2.385 ± 0.025	4.35±0.22
Plasmonic	1st	24.315 ± 0.015	0.255 ± 0.05	33.35 ± 0.12	2.053 ± 0.052	6.215 ± 0.085
	2nd	20.205 ± 0.135	0.225 ± 0.005	35.315 ± 0.325	1.6085 ± 0.0605	5.875 ± 0.005